ORIGINAL ARTICLE

ORAL DISEASES · WILEY

Notch activation leads to loss of myoepithelial differentiation and poor outcome in solid adenoid cystic carcinoma

Ye Zhang[1] | Xiaoxiao Liu[1] | Chuan-Xiang Zhou[1,2,3] | Tie-Jun Li[1,2,3] (iD)

[1]Department of Oral Pathology, Peking University School and Hospital of Stomatology, Beijing, PR China

[2]National Engineering Laboratory for Digital and Material Technology of Stomatology, Peking University School and Hospital of Stomatology, Beijing, PR China

[3]Research Unit of Precision Pathologic Diagnosis in Tumors of the Oral and Maxillofacial Regions, Chinese Academy of Medical Sciences (2019RU034), Beijing, PR China

Correspondence
Chuan-Xiang Zhou and Tie-Jun Li, Department of Oral Pathology, Peking University School and Hospital of Stomatology, Beijing, 100081, PR China.
Email: zhoucx2008@126.com (C.-X.Z.) and litiejun22@vip.sina.com (T.-J.L.).

Objective: We aimed to investigate Notch pathway dysregulation in solid adenoid cystic carcinoma (AdCC) and to define the association of Notch activation with cell differentiation and prognosis in AdCCs.

Materials and Methods: Notch1 mutations were detected from 125 AdCCs (62 cribriform-tubular; 63 solid). RNA-seq was performed in 16 AdCCs (6 Notch-mutant; 10 wild type). Notch activation indicator NICD and myoepithelial marker p63 were detected using immunohistochemistry and double-labelling immunofluorescence. The effect of exogenous NICD overexpression on p63 expression and cell proliferation was investigated using Western blotting and live-cell imaging.

Results: We identified 33 Notch1 activating mutations in 27 AdCCs including 26 solid and 1 cribriform-tubular subtypes. Six tumours harboured more than one Notch1 mutation, and 18 Notch1 mutations were novel. Most (47/63, 74.6%) solid AdCCs showed NICD overexpression, whereas 61 of 62 (98.4%) cribriform-tubular tumours were negative. NICD and p63 exhibited mutually exclusive expression, and exogenous NICD overexpression promoted cell proliferation and decreased p63 expression. NICD overexpression and Notch mutations were poor indicators for overall survival and metastasis, especially bone metastasis.

Conclusions: Dysregulated Notch signalling plays a critical role in AdCC severity. Notch activation may contribute to loss of myoepithelial differentiation as well as high proliferation and metastasis rates in solid AdCC.

KEYWORDS
activating mutation, adenoid cystic carcinoma, myoepithelial differentiation, Notch signalling pathway, poor outcome

1 | INTRODUCTION

Adenoid cystic carcinoma (AdCC) is one of the most common malignant tumours affecting salivary glands (Tian, Li, Wang, Hu, & Li, 2010). AdCC has an indolent growing pattern, but the long-term prognosis, mainly the solid type, is poor due to frequent local recurrence, distant metastasis and tendency for perineural invasion.

AdCC tumours exhibit biphasic differentiation of epithelial and myoepithelial cells with tubular, cribriform and solid growth patterns. Solid AdCC is considered a high-grade, more aggressive cancer with poorer prognosis than other subtypes (Du, Zhou, & Gao, 2016; Persson et al., 2009). Our previous study demonstrated that the cribriform or tubular subtype of AdCC predominantly consists of myoepithelial cells, whereas the solid growth pattern shows

luminal differentiation with loss of myoepithelial differentiation (Du et al., 2016). However, the molecular pathogenesis underlying the interplay of these subtypes or the formation of high-grade solid AdCC is poorly understood.

The Notch pathway is crucial for cellular morphogenesis. Notch receptor, ligands, DNA-binding transcription factor CSL, DNA-binding protein and regulators mediate stem/progenitor cell maintenance, proliferation, differentiation and apoptosis (Fortini, 2009). The Notch pathway is key for binary cell-fate decisions in mammary glands, with Notch activation promoting commitment to luminal rather than myoepithelial cell lineage (Bouras et al., 2008). Notch signalling is also critical for ductal cell differentiation in salivary glands (Dang et al., 2009). This pathway triggers a series of proteolytic cleavage events initiated through ligand binding. The activated form of Notch protein, the Notch intracellular domain (NICD), is generated through γ-secretase cleavage (Francis et al., 2002). After release and translocation to the nucleus, NICD forms a Notch transcription complex with the DNA-binding factor CSL, interacts with specific transcriptional factors and then activates downstream target genes (Nam, Weng, Aster, & Blacklow, 2003). Consequently, NICD expression is a vital indicator of Notch signalling activation (Ramakrishnan et al., 2012; Stoeck et al., 2014). Some patients with AdCC, who showed poor prognosis with distant metastasis, exhibited Notch1 mutations and diffuse NICD staining (Ferrarotto et al., 2017; Sajed et al., 2017).

Therefore, this study aimed to investigate Notch signalling pathway dysregulation in a large cohort of solid AdCCs. We examined Notch1 mutations and NICD expression in all AdCC subtypes and determined the possible relationship between activated Notch signalling and the characteristics of solid AdCC, especially the loss of myoepithelial differentiation and bone metastasis in tumour cells.

2 | MATERIALS AND METHODS

2.1 | Patients and tissue samples

This retrospective study reviewed cases diagnosed as AdCC from 2001 to 2017 in the files of Peking University School and Hospital of Stomatology and selected 125 cases. Slides were rereviewed by two senior pathologists in our department to ensure histological confirmation of the diagnosis and grading. Formalin-fixed, paraffin-embedded (FFPE) tumour samples (*n* = 125) were obtained for DNA sequencing, among which corresponding frozen tissues (*n* = 16) were available for RNA-based molecular analysis. Clinicopathologic variables were reviewed, including histological subtype, sex, age, disease site, T and N classification, clinical stage, recurrence, metastasis, survival status and treatment modality. Tumours were classified according to the World Health Organization's histological classification of salivary gland tumours (Stenman, Licitra, Said-Al-Naief, van Zante, & Yarbrough, 2017).

Patient follow-up data were obtained by reviewing medical records, telephone interviews and/or clinical examinations. Experiments and follow-up procedures of this study were approved by the University Institutional Ethics Committee (2017/NSFC/33), and the informed consent was obtained from patients.

2.2 | Mutation analysis after DNA extraction

The FFPE DNA Tissue Kit (Qiagen, Hilden, Germany) was used for standard genomic DNA extraction from FFPE samples, following the manufacturer's protocol. PCR was performed with 19 primer pairs (sequences in Table S1) covering 10 Notch1 coding exons (exons 25–34). Amplicons were subjected to Sanger sequencing (Beijing Genomics Institute, Beijing, China). Detected mutations were confirmed through reverse-sequencing and at least two more independent PCRs from the same samples. Mutations were validated through matched normal tissue sequencing (Table S3), and the novelty of Notch1 mutations was tested at cBioPortal (http://www.cbiopartal.org).

2.3 | Immunohistochemistry and immunostaining evaluation

A total of 125 FFPE samples of AdCC were obtained for immunohistochemistry. Serial sections (4 μm) were subjected to immunohistochemical staining using ChemMate Envision (Tsuneki et al., 2010). Primary antibodies (NICD, D3B8, 1:100, Cell Signaling Technology, Boston, USA; p63, 4A4, 1:250, Gene Tech, Shanghai, China; Ki-67, MIB1, 1:250, Gene Tech, Shanghai, China) were added to perform immunostaining. For negative control, the primary antibody was omitted and replaced with phosphate-buffered saline 1×. For positive control, sections of tumour tissues bearing activating Notch1 mutation in codon 2,467 that results in deletion of the C-terminal PEST degron domain were used for NICD immunostaining. The myoepithelial and basal cells in normal salivary gland tissues were used for p63 immunostaining. Images were acquired with Olympus microscope (BX51) and its matched camera (DP70) in ×200 magnification.

Two independent, blinded observers analysed the staining intensity and ratio of positive cells semiquantitatively. Reactivity was determined according to the percentage of positive cells: 0, up to 1%; 1, 2%–25%; 2, 26%–50%; 3, 51%–75%; and 4, over 75%. Intensity was graded as follows: 0, negative (no staining); 1, weakly positive; 2, moderately positive; and 3, strongly positive. The product of reactivity and intensity yielded a final score, graded as negative (0–1, −); weak (2–4, +); moderate (5–8, ++); and strong (9–12, +++) (Li, Zhou, & Gao, 2015). According to the immunostaining score, negative and weak staining were defined as low expression, while moderate and strong staining were defined as high expression (overexpression).

2.4 | Double-labelling immunofluorescence

The same slide was used for in situ detection of NICD and p63 with DAPI. Same as regular IHC's protocol, slides were deparaffinized and rehydrated, antigen retrieval and blocked. Primary monoclonal antibodies against NICD (D3B8, rabbit, monoclonal antibody, 1:100, Cell Signaling Technology) and p63 (4A4, 1:250, Gene Tech) were incubated at 4°C overnight. Slides were incubated sequentially with HRP-conjugated secondary antibodies for 30 min at room temperature, followed by tyramide-based HRP activation for 2 min. The secondary antibodies were anti-rabbit Envision reagent (Dako, Santa Clara, USA) and anti-mouse Envision reagent (Dako). HRP activators were biotinylated Fluorescein amplification reagent (1:50, PerkinElmer, Boston, USA) and Cyanine 3 amplification reagent (1:50, PerkinElmer), respectively. Images were acquired by confocal laser scanning microscopy.

2.5 | Plasmid transfection, cell proliferation and protein expression

AdCC cell line SACC-83 and NICD plasmid were obtained from the Department of Central Laboratory, Peking University School and Hospital of Stomatology, and the authenticity and purity of SACC-83 were confirmed by short tandem repeat analysis comparing DNA fingerprinting of SACC-83 with HeLa cells (Dong et al., 2011; Yang et al., 2017). Cells were incubated in RPMI 1640 medium (Gibco, Waltham, USA) containing 10% foetal bovine serum at 37°C and 5% CO_2. Cells were transfected with plasmids (NICD and empty vector) using Lipofectamine 3000 reagent (Invitrogen, Waltham, USA) and seeded in 96-well plate. The plate was monitored in real time every 3 hr from 0 to 60 hr with the IncuCyte ZOOM Live-Cell Imaging system (Essen Bioscience, Ann Arbor, USA). The percentage of cell confluence was calculated over time.

Cells were harvested at 72 hr post-transfection. Whole-cell proteins were extracted, subjected to 12% SDS-PAGE and then transferred onto a PVDF membrane (Millipore, Waltham, USA). Membranes were blocked and shaken at 4°C overnight with primary antibodies (β-actin, 1:1,000, Santa Cruz Biotechnology, Texas, USA; NICD, 1:1,000, Cell Signaling Technology; DeltaN p63, E6Q3O, 1:1,000, Cell Signaling Technology). After incubation of secondary antibodies (Cell Signaling Technology), immunoreactive proteins were detected using an enhanced chemiluminescence reagent (CW Bio, Beijing, China).

2.6 | Statistical analysis

Survival data were collected from a systematic follow-up database. All analyses were performed in SPSS 16.0. For immunostaining data, Pearson chi-square and Spearman's rank correlation tests were performed to compare the variables between groups. Recurrence-free survival was defined as the duration from the date of surgery to recurrence. Metastasis-free survival was defined as the duration from the surgery date to metastasis. Overall survival time was calculated the date of diagnosis to the date of AdCC-related death or follow-up cut-off date (31 December 2017). Five- and ten-year survival rates, as well as survival curves, were estimated using the Kaplan–Meier method and compared using log-rank tests. The Cox proportional hazards model was used to test the independent prognosis factors for OS. Potential prognostic factors were identified by univariate analysis, and significant variables were further analysed in the multivariate analysis. All tests were two-sided. A p value ≤ .05 was considered statistically significant.

3 | RESULTS

3.1 | Clinical and pathological profiles

Table 1 summarizes the clinicopathologic characteristics of 125 patients. All cases were presented in individuals with 62 cribriform-tubular and 63 solid variants. Women (69/125, 55.2%) had slightly higher incidence than men. The mean first-onset age was 49 (range: 19–75). The main primary tumours were more frequently located in the palatal gland (65/125, 52%). Other lesions were presented in the sublingual gland (29/125, 23.2%), submandibular gland (17/125, 13.6%), parotid gland (8/125, 6.4%) and cheek area (6/125, 4.8%). Solid variants were more likely to occur at the palate. Mean tumour size was 2.87 cm (range: 0.8–6.0 cm). More patients presented with T classification 3/4 (78/125, 62.4%), N classification 0/1 (110/125, 88%) and clinical stage III/IV (90/125, 72%) disease. Less than half (54/123, 43.9%) patients developed disease relapse. In 64 patients exhibited metastases, lung was the most common metastasis site, and other sites such as the bone and liver tissue were involved, especially for solid subtypes (p = .000 in the bone). Mortality rate was higher in solid subtypes (18/61, 29.5%) than cribriform-tubular types (36/62, 58.1%). Most (124/125, 99.2%) patients received surgery operation, and 93 patients went on postoperative therapy, including 80 with adjuvant radiation therapy only, 3 with adjuvant chemotherapy only and 10 with radiotherapy plus chemotherapy.

3.2 | Notch1 mutations in AdCC occurred at two hotspot regions associated with pathway activation

Sanger sequencing identified 33 Notch1 mutations in 27 patients, with six patients harbouring two Notch1 mutation, which exhibited 26 single-occurrence mutations and 3 recurrent mutations (Figure 1, Table S2). Furthermore, we confirmed 18 Notch1 mutations as novel mutations. Detected Notch1 mutations were mainly concentrated at two hotspot regions: negative regulatory region (NRR) and Pro-Glu-Ser-Thr-rich (PEST) domain (Figure 1). Because the physical dissociation of the Notch extracellular domain is linked to receptor activation, many gain-of-function mutations occur at the NRR (Rand et al., 2000; Sanchez-Irizarry et al., 2004). Additionally, the "PEST"

TABLE 1 Clinicopathologic characteristics of 125 patients with adenoid cystic carcinoma

Characteristics	Total	Cribriform-tubular	Solid
Sex			
Male	56	27 (48.2)	29 (51.8)
Female	69	35 (50.7)	34 (49.3)
Age (year)			
<60	98	52 (53.1)	46 (46.9)
≥60	27	9 (33.3)	18 (66.7)
Disease site			
Palatal gland	65	25 (38.5)	40 (61.5)
Sublingual gland	29	20 (69.0)	9 (31.0)
Submandibular gland	17	7 (41.2)	10 (58.8)
Parotid gland	8	4 (50.0)	4 (50.0)
Cheek area	6	5 (83.3)	1 (16.7)
T classification			
1/2	47	27 (57.4)	20 (42.6)
3/4	78	35 (44.9)	43 (55.1)
N classification			
0/1	110	58 (52.7)	52 (47.3)
2/3	15	4 (26.7)	11 (73.3)
Clinical stage at diagnosis			
I/II	35	20 (57.1)	15 (42.9)
III/IV	90	42 (46.7)	48 (53.3)
Disease recurrence			
No relapse	69	33 (47.8)	36 (52.2)
Relapse	54	28 (51.9)	26 (48.1)
Not known	2	1 (50.0)	1 (50.0)
Disease metastasis			
Distant metastasis	64	27 (42.2)	37 (57.8)
Lung	47	26 (55.3)	21 (44.7)
Bone	25	3 (12.0)	22 (88.0)
Liver	7	2 (28.6)	5 (71.4)
Others	5	1 (20.0)	4 (80.0)
Survival statue			
Alive	68	43 (63.2)	25 (36.8)
Dead	55	18 (32.7)	37 (67.3)
Not known	2	1 (50.0)	1 (50.0)
Treatment modality to the primary tumour			
No treatment	1	0	1 (100.0)
Surgery only	31	17 (54.8)	14 (45.2)
Surgical resection and postoperative therapy			
Radiotherapy only	80	40 (50.0)	40 (50.0)
Chemotherapy only	3	1 (33.3)	2 (66.7)
Radiotherapy plus chemotherapy	10	3 (30.0)	7 (70.0)

sequence targets NICD for degradation, and thus, PEST mutations, that mostly were short insertions or deletions causing shifts in the reading frame, lead to increased protein expression of NICD and activity (Weng et al., 2004).

It was noted that Notch1 mutations were defined in 41.3% (26/63) solid tumours and 1.6% (1/62) cribriform-tubular subtypes. Only one cribriform-tubular AdCC was found harbouring Notch1 mutation, which showed a predominant tubular pattern with a solid component representing no more than 30% of the tumour. All the other Notch1-mutant tumours were solid subtypes. This finding indicated that Notch1 mutations were associated with the solid growth pattern of AdCC.

3.3 | Diffuse NICD immunostaining correlated with Notch1 activating mutations, solid subtype and the loss of myoepithelial differentiation in AdCC

Representative histological (Figure 2a–d) and immunohistochemical (Figure 2e–l) images are shown in Figure 2. Most (61/62, 98.4%) cribriform-tubular tumours were negative for NICD, or else only a subset of cells was stained (Figure 2e, f), while 47 of 63 (74.6%) solid growth AdCCs were strongly positive for NICD (Figure 2g). Normal salivary gland tissue was negative for NICD (Figure 2h). On the contrary, p63 staining was positive in cribriform and tubular-type AdCC (Figure 2i, j), mainly at the periphery of cribriform arrangements and non-luminal cells of two-layered tubular structures, while its expression obviously decreased in solid AdCC (Figure 2k). P63 immunoreactivity was also detected in the myoepithelial and basal cells in normal gland tissue (Figure 2l). Furthermore, we found that NICD overexpression was significantly negatively correlated with that of myoepithelial marker p63 (Table 2, Figure 2e–l), implying the relationship of Notch activation with the loss of myoepithelial differentiation in AdCC. Furthermore, all 27 patients with Notch1 activating mutations exhibited high NICD expression (Table 2, Table S2), among which 26 were solid subtypes and one was defined as a cribriform-tubular subtype, showing a predominant cribriform-tubular pattern with a solid component representing no more than 30% of the tumour. This case with a mixture of tubular and solid growth patterns showed NICD overexpression (Figure 3a–c). Our findings revealed that diffuse NICD immunostaining is significantly correlated with Notch1 activating mutations, solid growth pattern and loss of myoepithelial differentiation marked by p63.

3.4 | Notch activation contributed to loss of myoepithelial differentiation and enhancement of proliferation in AdCC

We investigated the association of NICD expression with myoepithelial differentiation in 125 AdCCs and found that NICD staining
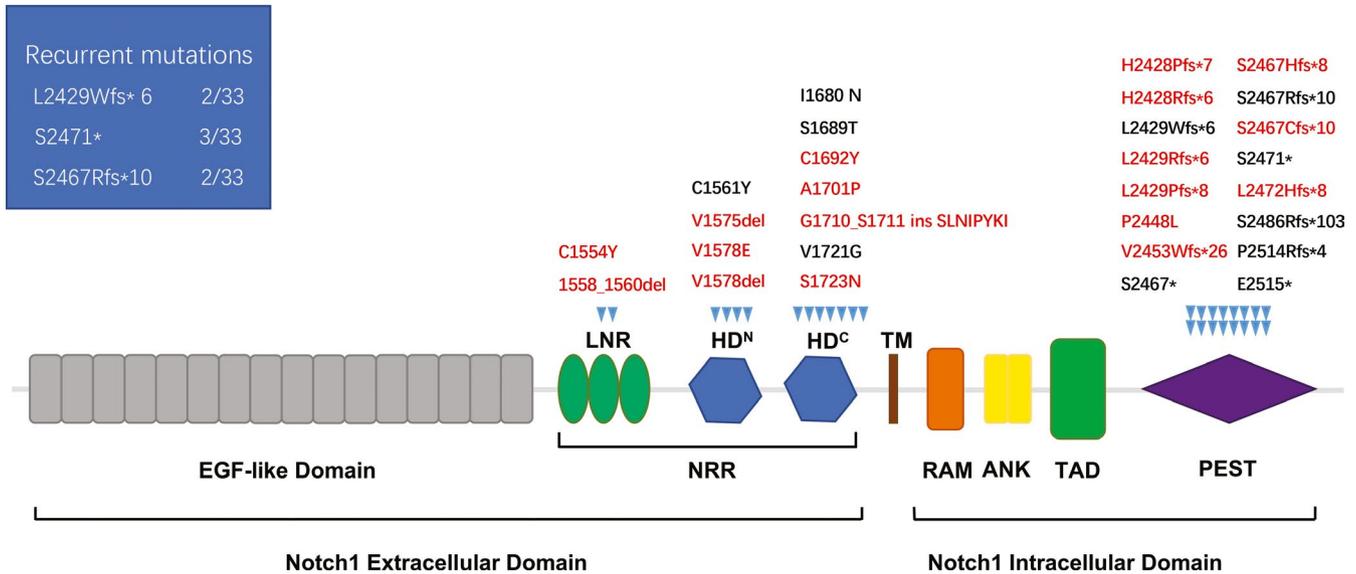
FIGURE 1 Sketch map of Notch1 mutations identified in AdCC. A schematic representation of human Notch1 mutations shows the distribution and frequency of NRR and PEST domain mutations in primary AdCC samples (blue triangles). Novel mutations (red words) and classic mutations (black words) are presented above. Recurrent mutations are shown at the left panel. Abbreviations: LNR, Lin/Notch repeats; HD-N and HD-C, N-terminal and C-terminal halves of the heterodimerization domain respectively; NRR, negative regulatory region; TM, transmembrane domain; RAM, RAM domain; ANK, ankyrin repeat domain; TAD, transcriptional activation domain, PEST, Pro-Glu-Ser-Thr-rich domain [Colour figure can be viewed at wileyonlinelibrary.com]

was significantly negatively associated with expression of myoepithelial marker p63 ($R = -.685$, $p = .000$), and they tended to exhibit mutually exclusive expression in luminal and myoepithelial cells (Figure 2). NICD expression was observed only in luminal epithelial cells, whereas p63 staining was conspicuously absent from them, instead of being visible at the periphery of cribriform arrangements and non-luminal cells of two-layered tubular structures. Immunofluorescence double-labelling assays with NICD and p63 confirmed the immunohistochemical findings by showing mutually exclusive expression of NICD and p63 in luminal and myoepithelial cells (Figure 3a–g).

To further investigate the effect of Notch activation on myoepithelial differentiation and proliferation of tumour cells in AdCC, we analysed the cell proliferation rate and p63 expression using the IncuCyte ZOOM Live-Cell Imaging system and Western blotting after introduction of exogenous NICD in AdCC. We found the introduction of exogenous NICD in AdCC tumour cells significantly downregulated p63 expression and, in the meantime, promoted cell proliferation (Figure 3h). Furthermore, the evident correlation of NICD overexpression with a high cell proliferation rate labelled by Ki-67 was found in AdCC specimens with a mixture of the cribriform and solid component (Figure 3i). The Ki-67 labelling index in different subtypes of AdCC revealed that solid tumours have a higher proliferation rate than cribriform-tubular tumours (Figure S1). Our findings indicated Notch activation contributes to loss of myoepithelial differentiation and promotion of cell proliferation in high-grade solid AdCC.

3.5 | Activating Notch1 mutation and NICD expression were associated with poor outcome of solid AdCC

In the 123 cases with follow-up data (2 patients' information was partially censored), median overall survival was 76 months (range: 4–192), with 57.3% at 5 y and 28.9% at 10 y. Kaplan–Meier analysis revealed that solid tumours result in poorer prognosis than other tumour subtypes ($p = .000$, Figure 4a). AdCCs with Notch1 activating mutations were associated with worse outcomes than the wild type ($p = .047$, Figure 4b). In addition, NICD overexpression was a poor prognostic indicator compared with the NICD low-expression group ($p = .000$, Figure 4c). In addition, univariable and multivariable Cox models were performed for OS (Table S4). Significant predictor variables by the univariable analysis were histological subtype, clinical stage, disease site, NICD staining and Notch1 mutational status. The subsequent multivariable analysis revealed that only histological subtype, clinical stage and NICD staining were significant predictors for OS. Notch1 mutation is not an independent prognosis factor when clinical stage, histology and NICD staining were considered. The significant association between Notch1 mutation and III/IV clinical stage ($p = .000$), solid type ($p = .000$) or NICD staining ($p = .000$) could dilute the prognostic significance of Notch1 mutation in the multivariable analysis. Median recurrence-free survival was 48 months (range: 3–147), while we did not identify significant differences in recurrence-free survival across mutation type, NICD staining outcome or histological subtype. Median metastasis-free survival was 66 months (range: 0–192), and
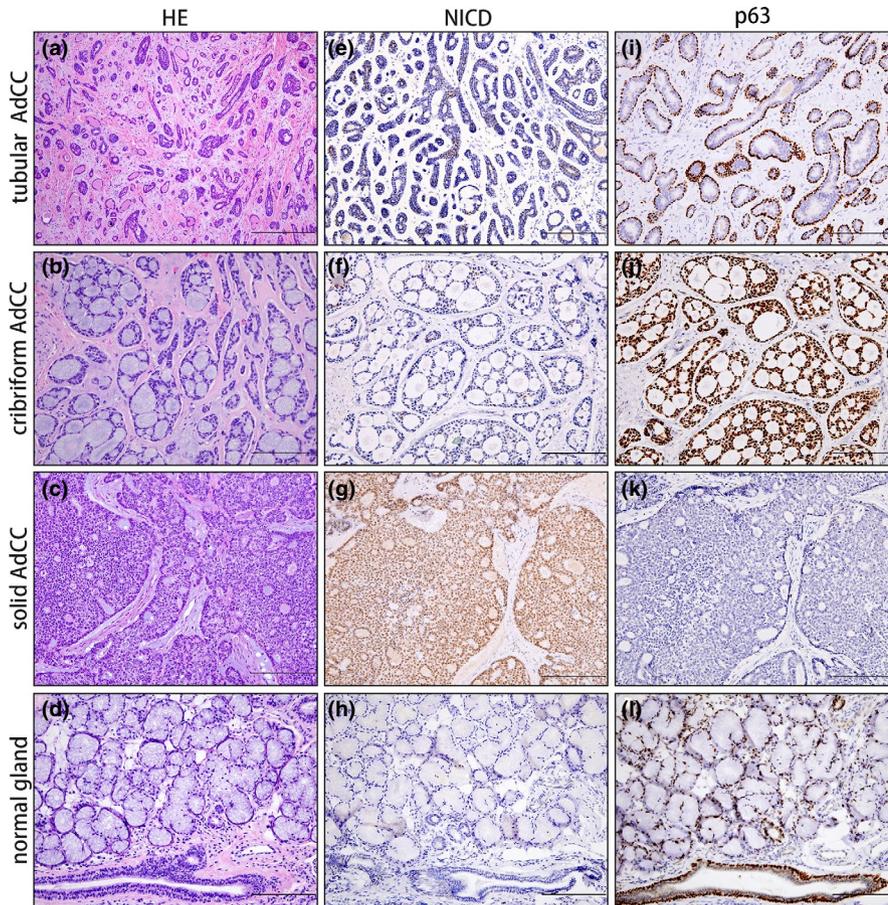
FIGURE 2 Representative immunohistochemical staining for NICD and p63 in different AdCC subtypes. Histological image of tubular (a), cribriform (b), solid (c) AdCC and normal salivary gland tissue (d). Negative NICD staining in tubular (e) and cribriform (f) subtype, diffusely positive NICD staining at luminal cell bulks in solid (g) subtype and normal salivary gland tissue was negative control for NICD (h). Positive p63 staining at the periphery of the non-luminal cells in tubular (i) and cribriform (j) subtype with negative NICD staining, negative p63 staining in majority of solid mass (k) and myoepithelial normal cells of salivary gland was positive control for p63 (l). The magnification of image (a–l) is ×200, scale bar 200 μm [Colour figure can be viewed at wileyonlinelibrary.com]

TABLE 2 Association of NICD expression with the histological subtype, Notch1 mutation and p63 staining in AdCC

Characteristics	NICD low expression[a] ($n = 77$)		NICD high expression[a] ($n = 48$)		Statistics[b]	
	No.	%	No.	%	X^2	p
Histological type					70.379	.000
Cribriform-tubular-	61	79.2	1	2.1		
Solid	16	20.8	47	97.9		
Notch1 mutation status					55.246	.000
Wild type	77	100	21	41.7		
Mutant type	0	0	27	58.3		
p63 staining					84.130	.000
Low expression[a]	8	10.4	45	93.75		
High expression[a]	69	89.6	3	6.25		

[a]According to the immunostaining score, negative and weak were defined as low expression, moderate and strong were defined as high expression.

[b]Pearson Chi-Square.

overexpression of NICD was significantly correlated with distant metastasis in AdCC ($p = .012$, Figure 4d).

Interestingly, we found that Notch1 mutation and NICD overexpression were significantly correlated with bone metastasis in AdCC (Figure 4e–f), but not with lung or other metastases. The results of PCA based on RNA-seq showed that 16 AdCC tumours fell into two major groups with 6 Notch-mutant and 10 wild-type

AdCCs exhibiting distinct gene expression signatures (Data S1). Compared to the wild-type AdCCs, Notch-mutant AdCCs exhibited upregulation of genes correlated with the osteoclast differentiation and bone metastasis, including AREG, Notch3, ANXA8, IRX1, HSD17B2, PRRX2, PTGIS, SHH, GPR132, TGFB2, MTA2, CHD7, KAT2A and SIM1, and the downregulation of genes involved in the osteoblast differentiation, including IGF2, SPARC,

FIGURE 3 Correlation of NICD overexpression with downregulation of p63 and upregulation of cell proliferation in AdCC. Histological (a) and immunofluorescence in situ detection of NICD and p63 (b, c) image of tubular–solid-combined AdCC subtype. Histological (d) and immunofluorescence in situ detection of NICD and p63 (e–g) image of cribriform–solid-combined AdCC subtype. The Cyanine 3 (red) marked NICD, the Fluorescein (green) is recognized for P63, and the DAPI (blue) marked nucleus. Western blotting analysis and proliferation analysis using IncuCyte ZOOM Live-Cell Imaging system in AdCC tumour cells with or without the introduction of exogenous NICD (h). Representative photo of immunostaining for Ki-67 (i) in cribriform-solid-combined AdCC. The magnification of image (a, b, d, e, i) is ×100, the magnification of image (c, f, g) is ×200, scale bar 200 μm [Colour figure can be viewed at wileyonlinelibrary.com]
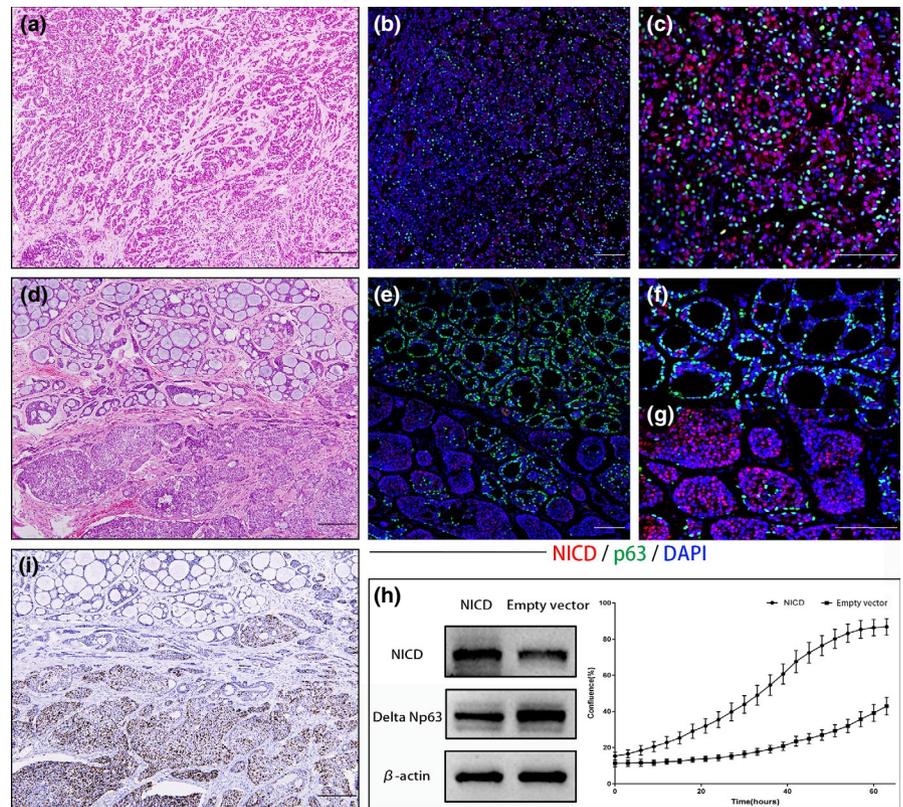
COL7A1 and COL17A1, and myoepithelial differentiation such as TP63 and KRT14 (Figure S2).

4 | DISCUSSION

Our previous study demonstrated that tumour cells in solid AdCC subtypes show luminal differentiation but loss of myoepithelial differentiation compared with the less aggressive cribriform-tubular AdCC (Du et al., 2016). It has been demonstrated by others that Notch activation drives luminal epithelial fate by downregulating TP63-mediated myoepithelial differentiation during development (Dang et al., 2009). Therefore, we hypothesize that Notch activation might tip the balance towards a luminal epithelial fate and a solid growth pattern in AdCC. Herein, we showed that most (47/63, 74.6%) solid AdCCs were diffusely positive for NICD, a vital indicator of Notch activation, while 61 of 62 (98.4%) cribriform-tubular tumours were negative for NICD, or else only a subset of cells was stained. In the meantime, we identified 33 Notch1 activating mutations in 27 patients, including 18 novel Notch1 mutations, which were concentrated in the NRR (exons 25–27) and PEST (exon 34) domains. Mutations in the former hotspot disrupt a negative regulatory region and trigger ligand-independent Notch1 activation. Mutations in the latter hotspot create premature stop codons on Notch1 protein with continual NICD stabilization, leading to pathway activation. As expected, Notch1 mutations were significantly associated with positive NICD in our study. All 27 tumours with Notch1 activating mutations exhibited NICD overexpression, among which 26 were

solid subtypes and one was defined as a cribriform-tubular subtype. This cribriform-tubular AdCC showed a mixture of tubular and solid patterns, with a less than 30% solid component, and NICD overexpression. Our findings indicate NICD overexpression is significantly correlated with Notch1 activating mutations and solid histology in AdCC.

Subsequently, we demonstrated that NICD and p63 had mutually exclusive expression in luminal and myoepithelial cells in both cribriform-tubular and solid tumours. Specifically, NICD expression was present only in luminal epithelial cells, whereas p63 expression was observed at the periphery of cribriform arrangements and non-luminal cells. Furthermore, exogenous NICD overexpression in AdCC tumour cells led to p63 downregulation. This mutual exclusivity of NICD and p63 is in line with previous studies, implicating Notch signalling in restricting bipotential progenitors to a luminal cell fate and TP63 as a determinant of basal/myoepithelial cell type under negative Notch control (Bouras et al., 2008; Dang et al., 2009; Drier et al., 2016; Yalcin-Ozuysal et al., 2010). In the meantime, PCA based on RNA-seq showed that AdCC tumours fell into two major groups with Notch-mutant and wild-type AdCCs exhibiting distinct gene expression signatures, and myoepithelial markers TP63 and KRT14 were found downregulated in Notch-mutant group. Furthermore, exogenous NICD overexpression in AdCC tumour cells promoted tumour cell proliferation, which was consistent with the higher cell proliferation rate found in solid AdCC patients with NICD overexpression labelled by Ki-67. Our findings indicate Notch activation contributes to the loss of myoepithelial differentiation and cell proliferation in high-grade, solid AdCC.
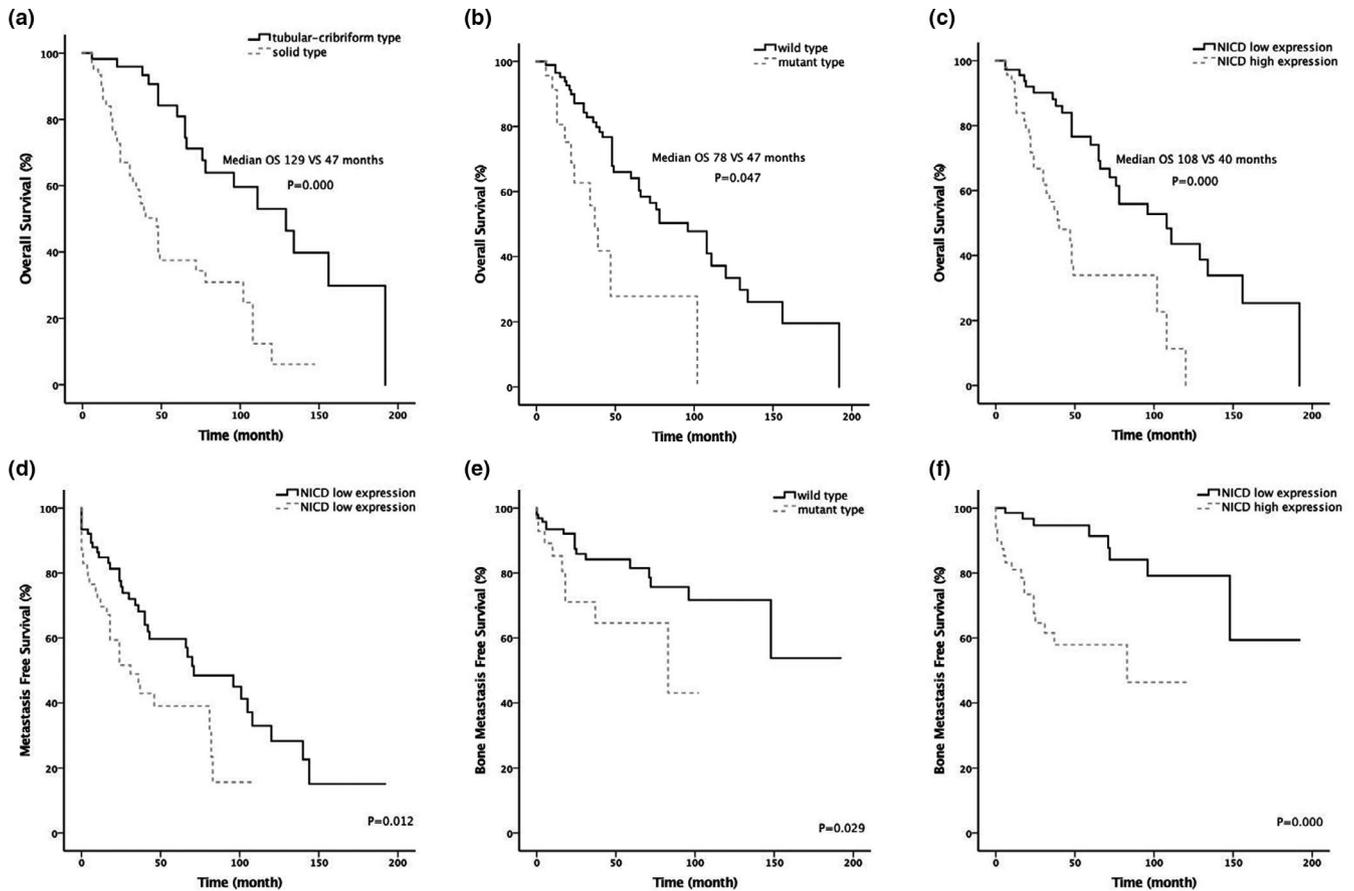
FIGURE 4 Survival situation under different group categorification. Kaplan–Meier analysis of overall survival with histological subtype (a), Notch mutational status (b) and NICD expression (c); Kaplan–Meier analysis of distant metastasis with NICD expression (d); Kaplan–Meier analysis of bone metastasis with Notch mutational status (e); and NICD expression (f)

In addition, potential prometastatic and poor prognostic role of NICD overexpression in AdCC suggests that the pathway may be an oncogenic target. We identified a significant association between NICD overexpression and distant AdCC metastasis. In previous studies, Notch1 mutations were more frequent in recurrent/metastatic AdCCs and were associated with distant metastases to the liver, bone and other atypical sites, rather than the more common AdCC metastasis sites such as lungs (Ferrarotto et al., 2017; Ho et al., 2019). Interestingly, comparing with wild-type AdCCs, Notch-mutant AdCCs exhibited upregulation of genes associated with osteoclast differentiation and bone metastasis, including AREG, Notch3, ANXA8, IRX1, HSD17B2, PRRX2, PTGIS, SHH, GPR132, TGFB2, MTA2, CHD7, KAT2A and SIM1, and the downregulation of genes involved in the osteoblast differentiation, including IGF2, SPARC, COL7A1 and COL17A1, based on RNA-seq analysis. Previous research demonstrated that Notch signalling stimulates osteogenesis, with continuous activation of the pathway linked to osteopenia in adult mice; the mechanism appears to involve impaired differentiation of mesenchymal stem cells into osteocytes (Ji, Ke, & Gao, 2017). Increased Notch1 expression has been reported in osteonectin-null osteoblasts (Kessler & Delany, 2007). These findings corroborate our results

of Kaplan–Meier analysis that revealed significantly higher bone metastasis proliferation rate in AdCCs with NICD overexpression. With limited data, our findings indicate that Notch pathway activation in solid AdCC might contribute to bone invasion and metastasis, and further research is required to clarify the underlying mechanisms, including large cohorts enrolled together with functional studies.

In summary, our findings provide important evidence regarding the critical role of dysregulated Notch signalling in AdCC severity. Although more research is required to clarify the genetic mechanism of intratumour heterogeneity and the pathogenesis of tumour progression in AdCC, we showed that Notch pathway activation may contribute to the loss of myoepithelial cell differentiation, as well as to higher proliferation and metastasis rates in solid AdCCs.

AUTHOR CONTRIBUTION

Ye Zhang: Data curation; Investigation; Software; Validation; Writing-original draft. **Xiaoxiao Liu:** Investigation; Validation. **Chuanxiang Zhou:** Conceptualization; Data curation; Funding acquisition; Methodology; Project administration; Supervision; Validation; Writing-review & editing. **Tiejun Li:** Conceptualization; Funding acquisition; Methodology; Project administration; Supervision; Validation; Writing-review & editing.

ORCID

Tie-Jun Li https://orcid.org/0000-0001-5983-2985

REFERENCES

Bouras, T., Pal, B., Vaillant, F., Harburg, G., Asselin-Labat, M.-L., Oakes, S. R., ... Visvader, J. E. (2008). Notch signaling regulates mammary stem cell function and luminal cell-fate commitment. *Cell Stem Cell*, 3, 429–441. https://doi.org/10.1016/j.stem.2008.08.001

Dang, H., Lin, A. L., Zhang, B., Zhang, H. M., Katz, M. S., & Yeh, C. K. (2009). Role for Notch signaling in salivary acinar cell growth and differentiation. *Developmental Dynamics*, 238(3), 724–731. https://doi.org/10.1002/dvdy.21875

Dong, L., Wang, Y. X., Li, S. L., Yu, G. Y., Gan, Y. H., Li, D., & Wang, C. Y. (2011). TGF-beta1 promotes migration and invasion of salivary adenoid cystic carcinoma. *Journal of Dental Research*, 90(6), 804–809. https://doi.org/10.1177/0022034511401407

Drier, Y., Cotton, M. J., Williamson, K. E., Gillespie, S. M., Ryan, R. J. H., Kluk, M. J., ... Bernstein, B. E. (2016). An oncogenic MYB feedback loop drives alternate cell fates in adenoid cystic carcinoma. *Nature Genetics*, 48, 265–272. https://doi.org/10.1038/ng.3502

Du, F., Zhou, C. X., & Gao, Y. (2016). Myoepithelial differentiation in cribriform, tubular and solid pattern of adenoid cystic carcinoma: A potential involvement in histological grading and prognosis. *Annals of Diagnostic Pathology*, 22, 12–17. https://doi.org/10.1016/j.anndiagpath.2016.03.001

Ferrarotto, R., Mitani, Y., Diao, L., Guijarro, I., Wang, J., Zweidler-McKay, P., ... Kapoun, A. M. (2017). Activating NOTCH1 mutations define a distinct subgroup of patients with adenoid cystic carcinoma who have poor prognosis, propensity to bone and liver metastasis, and potential responsiveness to Notch1 inhibitors. *Journal of Clinical Oncology*, 35(3), 352. https://doi.org/10.1200/JCO.2016.67.5264

Fortini, M. E. (2009). Notch signaling: The core pathway and its post-translational regulation. *Developmental Cell*, 16(5), 633–647. https://doi.org/10.1016/j.devcel.2009.03.010

Francis, R., McGrath, G., Zhang, J., Ruddy, D. A., Sym, M., Apfeld, J., ... Curtis, D. (2002). Aph-1 and pen-2 are required for Notch pathway signaling, γ-secretase cleavage of βAPP, and presenilin protein accumulation. *Developmental Cell*, 3(1), 85–97. https://doi.org/10.1016/s1534-5807(02)00189-2

Ho, A. S., Ochoa, A., Jayakumaran, G., Zehir, A., Valero Mayor, C., Tepe, J., ... Morris, L. G. T. (2019). Genetic hallmarks of recurrent/metastatic adenoid cystic carcinoma. *The Journal of Clinical Investigation*, 129(10), 4276–4289. https://doi.org/10.1172/JCI128227

Ji, Y., Ke, Y., & Gao, S. (2017). Intermittent activation of notch signaling promotes bone formation. *American Journal of Translational Research*, 9(6), 2933. PMID: 28670381 (NO doi).

Kessler, C. B., & Delany, A. M. (2007). Increased Notch 1 expression and attenuated stimulatory G protein coupling to adenylyl cyclase in osteonectin-null osteoblasts. *Endocrinology*, 148(4), 1666–1674. https://doi.org/10.1210/en.2006-0443

Li, Y. Y., Zhou, C. X., & Gao, Y. (2015). Moesin regulates the motility of oral cancer cells via MT1- MMP and E-cadherin/p120-catenin adhesion complex. *Oral Oncology*, 51, 935–943. https://doi.org/10.1016/j.oraloncology.2015.07.003

Nam, Y., Weng, A. P., Aster, J. C., & Blacklow, S. C. (2003). Structural requirements for assembly of the CSL intracellular Notch1. Mastermind-like 1 transcriptional activation complex. *Journal of Biological Chemistry*, 278(23), 21232–21239. https://doi.org/10.1074/jbc.M301567200

Persson, M., Andren, Y., Mark, J., Horlings, H. M., Persson, F., & Stenman, G. (2009). Recurrent fusion of MYB and NFIB transcription factor genes in carcinomas of the breast and head and neck. *Proceedings of the National Academy of Sciences*, 106(44), 18740–18744. https://doi.org/10.1073/pnas.0909114106

Ramakrishnan, V., Ansell, S., Haug, J., Grote, D., Kimlinger, T., Stenson, M., ... Kumar, S. (2012). MRK003, a γ-secretase inhibitor exhibits promising in vitro pre-clinical activity in multiple myeloma and non-Hodgkin's lymphoma. *Leukemia*, 26(2), 340. https://doi.org/10.1038/leu.2011.192

Rand, M. D., Grimm, L. M., Artavanis-Tsakonas, S., Patriub, V., Blacklow, S. C., Sklar, J., & Aster, J. C. (2000). Calcium depletion dissociates and activates heterodimeric notch receptors. *Molecular and Cellular Biology*, 20(5), 1825–1835. https://doi.org/10.1128/mcb.20.5.1825-1835.2000

Sajed, D. P., Faquin, W. C., Carey, C., Severson, E. A., H. Afrogheh, A., A. Johnson, C., ... Aster, J. C. (2017). Diffuse staining for activated NOTCH1 correlates with NOTCH1 mutation status and is associated with worse outcome in adenoid cystic carcinoma. *The American Journal of Surgical Pathology*, 41(11), 1473. https://doi.org/10.1097/PAS.0000000000000945

Sanchez-Irizarry, C., Carpenter, A. C., Weng, A. P., Pear, W. S., Aster, J. C., & Blacklow, S. C. (2004). Notch subunit heterodimerization and prevention of ligand-independent proteolytic activation depend, respectively, on a novel domain and the LNR repeats. *Molecular and Cellular Biology*, 24(21), 9265–9273. https://doi.org/10.1128/mcb.24.21.9265-9273.2004

Stenman, G., Licitra, L., Said-Al-Naief, N., van Zante, A., & Yarbrough, W. G. (2017). Tumours of the salivary glands. In A. K. El Naggar, J. K. C. Chan, J. R. Grandis, T. Takata, & P. J. Slootweg (Eds.), *World Health Organization classification of head and neck tumours* (pp. 164–165). Lyon: IARC Press.

Stoeck, A., Lejnine, S., Truong, A., Pan, L., Wang, H., Zang, C., ... Sathyanarayanan, S. (2014). Discovery of biomarkers predictive of GSI response in triple-negative breast cancer and adenoid cystic carcinoma. *Cancer Discovery*, 4(10), 1154–1167. https://doi.org/10.1158/2159-8290.CD-13-0830

Tian, Z., Li, L., Wang, L., Hu, J., & Li, J. (2010). Salivary gland neoplasms in oral and maxillofacial regions: A 23-year retrospective study of 6982 cases in an eastern Chinese population. *International Journal of Oral and Maxillofacial Surgery*, 39(3), 235–242. https://doi.org/10.1016/j.ijom.2009.10.016

Tsuneki, M., Yamazaki, M., Cheng, J., Maruyama, S., Kobayashi, T., & Saku, T. (2010). Combined immunohistochemistry for the differential diagnosis of cystic jaw lesions: Its practical use in surgical pathology. *Histopathology*, 57, 806–813. https://doi.org/10.1111/j.1365-2559.2010.03712.x

Weng, A. P., Ferrando, A. A., Lee, W., Morris, J. P., Silverman, L. B., Sanchez-Irizarry, C., ... Aster, J. C. (2004). Activating mutations of NOTCH1 in human T cell acute lymphoblastic leukemia. *Science*, 306(5694), 269–271. https://doi.org/10.1126/science.1102160

Yalcin-Ozuysal, Ö., Fiche, M., Guitierrez, M., Wagner, K. U., Raffoul, W., & Brisken, C. (2010). Antagonistic roles of Notch and p63 in controlling mammary epithelial cell fates. *Cell Death and Differentiation*, 17(10), 1600. https://doi.org/10.1038/cdd.2010.37

Yang, W.-W., Yang, L.-Q., Zhao, F., Chen, C.-W., Xu, L.-H., Fu, J., … Ge, X.-Y. (2017). Epiregulin promotes lung metastasis of salivary adenoid cystic carcinoma. *Theranostics*, *7*(15), 3700–3714. https://doi.org/10.7150/thno.19712

SUPPORTING INFORMATION

Additional supporting information may be found online in the Supporting Information section.